A MODEL OF RESPIRATORY HEAT TRANSFER IN A SMALL MAMMAL

J. C. COLLINS, T. C. PILKINGTON, *and* K. SCHMIDT-NIELSEN

From the Departments of Biomedical Engineering and Zoology, Duke University, Durham, North Carolina 27706. Dr. Collins' present address is the Department of Electrical Engineering, University of Kentucky, Lexington, Kentucky 40506.

ABSTRACT A steady-state model of the heat and water transfer occurring in the upper respiratory tract of the kangaroo rat, *Dipodomys spectabilis*, is developed and tested. The model is described by a steady-state energy balance equation in which the rate of energy transfer from a liquid stream (representing the flow of heat and blood from the body core to the nasal region) is equated with the rate of energy transfer by thermal conduction from the nose tip to the environment. All of the variables in the equation except the flow rate of the liquid stream can be either measured directly or estimated from physiological measurements, permitting the solution of the equation for the liquid stream flow rate. After solving for the liquid stream flow rate by using data from three animals, the energy balance equation is used to compute values of energy transfer, expired air temperature, rates of water loss, and efficiency of vapor recovery for a variety of ambient conditions. These computed values are compared with values measured or estimated from physiological measurements on the same three animals, and the equation is thus shown to be internally consistent. To evaluate the model's predictive value, calculated expired air temperatures are compared with measured expired air temperatures of eight additional animals. Finally, the model is used to examine the general dependence of expired air temperature, of rates of water loss, and of efficiency of vapor recovery on ambient conditions.

INTRODUCTION

The background for this study is the remarkable water economy which enables kangaroo rats to survive in arid regions of the American Southwest. One aspect of this water economy is a very low rate of respiratory water loss, which is attributable to remarkably low temperatures in the air passages rather than to any unusual ability to reduce respiratory ventilation rate by an increased extraction of oxygen from the pulmonary air. The nasal passageways have been described as a heat exchanger in which during inspiration heat and water are added to the inspired air,

and during expiration part of the heat and water are redeposited on the now cooler walls (Jackson and Schmidt-Nielsen, 1964; Schmidt-Nielsen et al., 1970; Murrish and Schmidt-Nielsen, 1970).

In the present study we have developed a quantitative steady-state model for heat and water transfer in the upper respiratory tract based on the kangaroo rat, *D. spectabilis*, but presumably also applicable to other small mammals with a similar nasal geometry. The model can account for observed variations in expired air temperature and rate of water loss, and can predict values of these parameters as functions of ambient temperature and humidity.

LIST OF SYMBOLS

c	Specific heat, cal (g °C)$^{-1}$.
c_p	Specific heat of fluid at constant pressure, cal (g °C)$^{-1}$.
C	Fractional concentration of diffusing substance, nondimensional.
D	Diffusion coefficient, cm^2 sec^{-1}.
f_{resp}	Respiration frequency, sec^{-1}.
h	Surface heat transfer coefficient, cal (sec cm^2 °C)$^{-1}$.
H_i	Partial specific enthalpy of the ith component, cal g^{-1}.
$H_{v,\ ex}$	Enthalpy of water vapor at expired air temperature, cal g^{-1}.
$H_{w,b}$	Enthalpy of liquid water at body core temperature (T_b), cal g^{-1}.
$\mathbf{J}_i$	Barycentric mass flux, cal sec^{-1}.
$\mathbf{J}_q$	Total barycentric heat flux, cal sec^{-1}.
k	Thermal conductivity, cal (cm °C sec)$^{-1}$.
$[O_2]_a$	Oxygen fractional concentration of ambient air, nondimensional.
$[O_2]_A$	Mean oxygen fractional concentration of alveolar air, nondimensional.
$[O_2]_D$	Mean oxygen fractional concentration in the dead space at the beginning of inspiration, nondimensional.
$[O_2]_{\bar{L}}$	Mean oxygen fractional concentration of air entering the alveoli, nondimensional.
$\mathbf{q}$	Reduced heat flux, cal sec^{-1}.
$\dot{q}$	Heat transfer rate, cal sec^{-1}.
ΔT	Temperature difference, °C.
T_a	Ambient temperature, °C.
T_{ex}	Nose tip (expired air) temperature, °C.
V_A	Alveolar exchange volume, cm^3.
V_D	Physiological dead space, cm^3.
V_T	Tidal volume, cm^3.
$\dot{V}_a$	Ventilation rate, flow rate of airstream, g sec^{-1}.
$\dot{V}_l$	Effective flow rate of liquid stream, blood flow plus tissue heat flow, g sec^{-1}.
$\dot{V}_{O_2}$	Oxygen consumption rate, cm^3 sec^{-1}.
$[W]_a$	Absolute humidity of ambient air, nondimensional (g vapor/g dry air).
$[W]_b$	Absolute humidity of pulmonary air (saturated at T_b), nondimensional (g vapor/g dry air).
$[W]_{ex}$	Absolute humidity of expired air (saturated at T_{ex}), nondimensional (g vapor/g dry air).
β_{ij}	Phenomenological coefficients (units vary).
χ_k	Mass concentration gradient driving force, cm^{-1}.
χ_0	Thermal gradient driving force, cm^{-1}.

DEVELOPMENT OF THE MODEL

In general, mammals breathe in and out through the nose. Under normal conditions, an axial gradient will exist in the nasal passages, the temperature increasing with passage depth. When air flows in the passage, friction establishes a nonuniform velocity profile across the airstream. The axial thermal gradient and boundary layer effect thus establish a transverse thermal gradient, causing thermal diffusion across the boundary layer. During expiration, the directions of axial flow and of transverse thermal diffusion are reversed relative to the directions during inspiration.

During inspiration, water vapor diffuses from the boundary layer at the passage wall to the faster-moving core of air at the center of the stream and is replaced by evaporation at the wall. During expiration, vapor diffuses from the center of the stream to the boundary layer and is condensed on the wall. Furthermore, since expired air differs from environmental air in oxygen and carbon dioxide concentrations (because of gas exchange in the lungs), transverse diffusion of these components also occurs.

An exact analysis of these exchange processes in the nasal passages of the kangaroo rat is difficult because the distribution of blood flow and conductive heat flow from the body core to the nasal passages is complex. The cross-sectional configuration of the nasal passages of the kangaroo rat also changes rapidly with passage depth (Jackson and Schmidt-Nielsen, 1964), but the transverse dimension remains at about 0.3 mm (Collins, 1970).

The temperature at a given depth in the nasal passages depends primarily on the temperature and humidity of the ambient air. Lowering ambient temperature tends to lower nasal temperatures because of increased evaporative cooling of the passage walls during inspiration. In this study, the temperature at fixed positions in the nasal passages was monitored for periods of several hours on animals restrained under constant environmental conditions. Although activity (i.e., amount of struggling) varied considerably over such periods, the nasal temperatures did not in any case change more than 0.5°C over the entire period. Moreover, any drift was usually correlated with simultaneous drift in rectal temperature. Nasal temperatures in the kangaroo rat therefore appear to change primarily in response to changes in environmental conditions and not in response to changes in activity. This suggests that it is feasible to develop a quantitative model of nasal passage heat exchange relating respiratory parameters and environmental conditions.

Justification of a Steady-State Model

The purpose of the following discussion is to establish the validity of describing the net exchange of water vapor and heat in a steady-state, continuous flow system in place of analyzing the transient events during each inspiration and expiration. Thus, this section discusses the question of the extent to which air in the nasal passages can be expected to be in thermal and mass steady state with air at the passage walls.

Assume a channel model consisting of flat parallel plates maintained at a temperature T_1 and separated a distance of 0.3 mm. At some reference time, air at an initial temperature $T_2 \neq T_1$ is suddenly introduced into the space between the walls. If specific heat, thermal conductivity, and density are constant,

$$\nabla^2 T = \frac{\rho c}{k} \frac{\partial T}{\partial t} = \frac{1}{\alpha} \frac{\partial T}{\partial t}, \tag{1}$$

where T is temperature, t is time, k is thermal conductivity, ρ is density, and c is specific heat (Rohsenow and Choi, 1961). The general solution to this equation is

$$\frac{T - T_1}{T_2 - T_1} = 2 \sum_{n=1}^{\infty} \frac{\sin \lambda_n r_0}{\lambda_n r_0 + \sin \lambda_n r_0 \cos \lambda_n r_0} \exp(-\lambda_n^2 \alpha t) \cos \lambda_n y, \tag{2}$$

where y is the distance from the center line of the space to the point in question and λ_n are the roots of

$$\cot(\lambda_n r_0) = \frac{k}{h} \lambda_n, \tag{3}$$

r_0 is half the separation distance (0.15 mm), and h is the surface heat transfer coefficient, which for this geometry has been estimated to be 1.7×10^{-2} cal/(sec cm^2 °C) for air at 16°C (Rohsenow and Choi, 1961). Using these values of h and r_0 and assuming the thermal conductivity of air to be 6.2×10^{-5} cal(cm sec °C)$^{-1}$ permits solving equation 3 for λ_n. Under these conditions equation 2 becomes

$$\frac{T - T_1}{T_2 - T_1} \cong 1.23 \exp\left(\frac{-t}{0.676 \times 10^{-3}}\right) \cos 84.8y - 0.326 \exp\left(\frac{-t}{0.07 \times 10^{-3}}\right) \cos 263y + 0.143 \exp\left(\frac{-t}{0.023 \times 10^{-3}}\right) \cos 455y - \cdots \tag{4}$$

where y is in centimeters and t is in seconds. The solution is a sum of exponentially decaying terms which vary sinusoidally in space. The first term has the longest time constant (0.676×10^{-3} sec) and therefore determines how much time is required for thermal equilibrium to be approached.

Suppose now that the walls are wet and maintained at temperature T_1 and that at some reference time dry air, also at temperature T_1, is injected into the region between the walls. For isotropic media in which diffusion obeys the rate equation

$$\text{Mass flux} = -D \text{ (concentration gradient)}, \tag{5}$$

where D is the diffusion coefficient. For systems where D is independent of position and there is no production or immobilization of the diffusing material within the

system,

$$\nabla^2 C = \frac{1}{D}\frac{\partial C}{\partial t}, \tag{6}$$

where C is the concentration of the diffusing substance. If the system boundary is defined just inside the wall, all the criteria are approximately satisfied. It is assumed that evaporation at the wall is instantaneous. If sufficient water is available at the wall, this system is analogous to the system of equation 1, with vapor concentration analogous to temperature and the surface mass transfer coefficient, analogous to h in equation 3, assumed infinite (Rohsenow and Choi, 1961). The values of λ_n satisfying equation 3 in this case are

$$\lambda_n = \frac{(2n-1)\pi}{2r_0}, \qquad n = 1, 2, \cdots \tag{7}$$

Using properties for air and water vapor at 16°C, $D = 0.208$ cm²/sec, yields the following solution to equation 6:

$$\frac{C - C_1}{C_2 - C_1} = \frac{4}{\pi}\sum_{n=1}^{\infty}(-1)^{n+1}\left(\frac{1}{2n-1}\right)\exp\left(\frac{-(2n-1)^2 t}{0.379 \times 10^{-3}}\right) \cdot\cos\,[(2n-1)104.6y]. \tag{8}$$

This solution is analogous to equation 4, with the first ($n = 1$) term having the longest time constant and determining the time required for equilibrium to be approached. Since this time constant is less than the longest thermal time constant, the mass diffusion process of equation 8 should approach equilibrium somewhat more rapidly than the thermal diffusion system of equation 4.

Transverse oxygen and carbon dioxide gradients also exist in the nasal passages. Their diffusion through air can be treated in a manner analogous to that in which the diffusion of water vapor through air was treated. Assuming identical initial and boundary conditions, the solution analogous to equation 8 for air and carbon dioxide is

$$\frac{C - C_1}{C_2 - C_1} = \frac{4}{\pi}\sum_{n=1}^{\infty}(-1)^{n+1}\left(\frac{1}{2n-1}\right)\exp\left(\frac{-(2n-1)^2 t}{0.606 \times 10^{-3}}\right) \cdot\cos\,[(2n-1)104.6y]. \tag{9}$$

For air and oxygen, the analogous solution is

$$\frac{C - C_1}{C_2 - C_1} = \frac{4}{\pi}\sum_{n=1}^{\infty}(-1)^{n+1}\left(\frac{1}{2n-1}\right)\exp\left(\frac{-(2n-1)^2 t}{0.472 \times 10^{-3}}\right) \cdot\cos\,[(2n-1)104.6y]. \tag{10}$$

In both equation 9 and equation 10, the longest time constants are shorter than the thermal time constant of equation 4, implying that these mass diffusion processes would also approach equilibrium more rapidly than the pure thermal diffusion process.

Now assume that the channel walls are wet and maintained at temperature T_1 and that at some reference time a mass of air saturated with vapor at some temperature $T_2 > T_1$ is suddenly introduced into the region between the two walls. Simultaneous mass and thermal diffusion will occur, during which the air will be both lowered in vapor content and cooled.

The rate equations for the simultaneous processes are

$$\mathbf{q} = \beta_{00}\chi_0 + \sum_{k=1,2} \beta_{0k}\chi_k \quad \text{and} \tag{11}$$

$$\mathbf{J}_i = \beta_{i0}\chi_0 + \sum_{k=1,2} \beta_{ik}\chi_k . \tag{12}$$

$\mathbf{J}_i$ is the barycentric mass flux of the ith component (either air or water vapor), $\chi_0 \equiv -(\text{grad } T)/T$ is the thermal gradient driving force, β are the phenomenological coefficients, χ_k are the mass concentration gradient driving forces, and $\mathbf{q}$ is the reduced heat flux, defined as

$$\mathbf{q} = \mathbf{J}_q - \sum_{i=1,2} H_i \mathbf{J}_i , \tag{13}$$

where $\mathbf{J}_q$ is the total barycentric heat flux and H_i is the partial specific enthalpy of the ith component (Merk, 1958). Collins (1970) has developed a detailed argument which suggests that under typical physiological conditions the dependence of reduced heat flux on mass concentration gradients and that of mass flux on thermal gradients are negligible compared with the dependence of reduced heat flux on thermal gradient and that of mass flux on mass concentration gradient.

If transverse thermal and mass diffusion do occur independently, an estimate of the difference in temperature between the passage wall and the center of the air-stream under conditions of laminar axial convective flow may be obtained without considering mass effects if nominal flow conditions are known. If average values of tidal volume and respiration rate determined during this study are assumed, the average volumetric flow rate of air through the upper respiratory tract of the kangaroo rat is 2.10 cm³/sec. For many small animals, the peak rate of air flow is about twice the average rate (Guyton, 1947), leading to an estimated peak rate of 4.38 cm³/sec. Measurements made on a number of nasal passage casts during this study show the average cross-sectional area to be about 0.104 cm², which yields an estimated bulk-average peak velocity of about 42 cm/sec. The peak velocity of fully developed laminar flow between parallel flat plates is 1.5 times the average velocity (Schlichting, 1960), so that the estimated peak velocity of air in the nasal passages of the kangaroo rat is about 63 cm/sec if the parallel plate model of the nasal pas-

sages is assumed. The maximum axial thermal gradient encountered during this study was about 1.0°C/mm. Assuming such conditions and a Nusselt number of 8.22 (Rohsenow and Choi, 1961) in the parallel plate model of the nasal passages gives a temperature difference of 0.22°C between the wall and the center of the airstream (Rohsenow and Choi, 1961). Neglecting fluctuations in wall temperature, the maximum cyclical center line thermal fluctuation expected should be about twice this value (because of the tidal nature of respiratory flow), or less than 0.5°C. Observed cyclical fluctuations were always 0.3°C or less.

The foregoing analysis is a worst-case analysis, for the bulk-average conditions of air at any given depth are always closer to those at the wall than are the conditions of air at the center line. Laminar flow was assumed because the Reynolds number for 0.3 mm nasal passages and an air velocity of 60 cm/sec is less than 25 (Kays, 1966); however, turbinate structures (particularly pronounced at the exterior end of the passages) and entry effects facilitate transverse mixing. It may be concluded that approximate thermal and mass concentration equilibria should exist at any given depth in the nasal passages of the kangaroo rat.

Justification of Using a Single Flow to Replace Multiple Flows

The model developed in this paper utilizes one liquid stream to represent the flow of heat and blood from the body core to the nasal region. This section justifies this one-stream representation by showing that the single stream is equivalent to multiple streams.

Assume in Fig. 1 *a* a simple distributed flow heat exchanger consisting of two channels. Fluid enters the first channel at a rate $\dot{V}_1$ and a temperature T_1 and leaves at a lower temperature T_2. This exit is close enough to the entrance of the second channel so that fluid flowing at a rate $\dot{V}_2$ enters that channel at the same temperature T_2 and leaves at a still lower temperature T_3. In Fig. 1 *b*, the two channels have been replaced by a single channel in which fluid flowing at a rate $\dot{V}$ enters at temperature T_1 and leaves at temperature T_3. If the two systems are equivalent, the rates of heat transfer can be equated:

$$\dot{V}_1(T_1 - T_2)c_p + \dot{V}_2(T_2 - T_3)c_p \overset{?}{=} \dot{V}(T_1 - T_3)c_p, \tag{14}$$

where c_p is the specific heat of the fluid and is assumed to be constant. Solving equation 14 for $\dot{V}$ gives

$$\dot{V} \overset{?}{=} \frac{\dot{V}_1\Delta T_1 + \dot{V}_2\Delta T_2}{\Delta T_1 + \Delta T_2} = \frac{\sum_i \dot{V}_i \Delta T_i}{\sum_i \Delta T_i}, \tag{15}$$

where $\Delta T_1 = T_1 - T_2$, $\Delta T_2 = T_2 - T_3$, and ΔT_i is the temperature difference

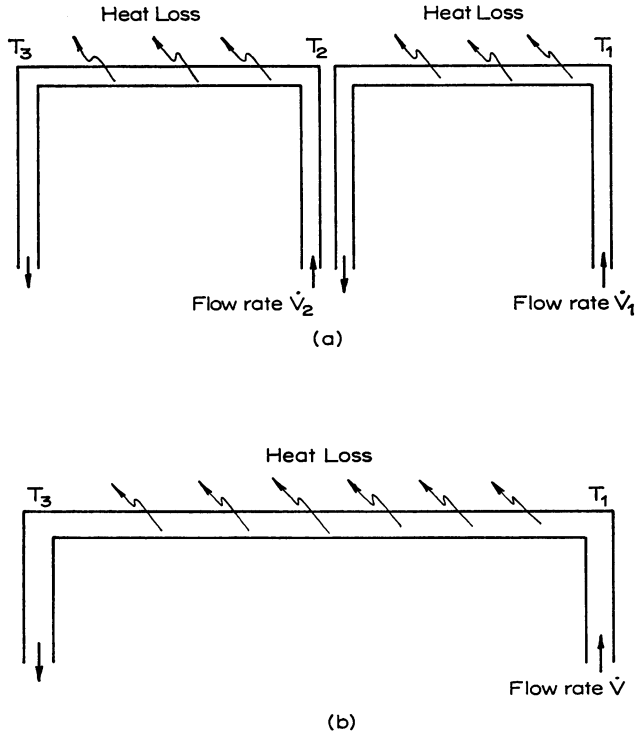

FIGURE 1 (*a*) Heat transfer from distributed flow system. (*b*) Representation of distributed flow of *a* by a single equivalent flow.

associated with the *i*th flow. Examination of equation 15 reveals that if $\dot{V}$ is selected as the weighted mean of $\dot{V}_1$ and $\dot{V}_2$ the rates of heat transfer are equal and the systems are equivalent.

This reasoning can be extended to replace any number of distributed flows by a single flow, the rate of which is the weighted mean of the component flow rates, whether the component flows overlap, are separated, transfer no heat, or actually extract heat from the system. For example, assume a system consisting of n separate flows of the same fluid. Let the first flow $\dot{V}_1$ enter the system at a temperature T_1 and the nth flow $\dot{V}_n$ leave at a temperature T_{n+1}. Nothing else is known about any of the flows. These flows are to be replaced by a single flow entering at temperature T_1 and leaving at temperature T_{n+1}. If the heat transferred by the two systems is to be the same, then

$$\dot{V}_1(T_1 - \cdots)c_p + \cdots + \dot{V}_i(T_j - T_k)c_p + \cdots + \dot{V}_n(\cdots - T_{n+1})c_p = \dot{V}(T_1 - T_{n+1})c_p . \quad (16)$$

Let the temperature difference associated with the *i*th flow be denoted by ΔT_i and

the difference associated with $\dot{V}$ by ΔT. Equation 16 can be solved for $\dot{V}$:

$$\dot{V} = \frac{\sum_i \dot{V}_i \Delta T_i}{\Delta T} = \sum_i \dot{V}_i \frac{\Delta T_i}{\Delta T} = \sum_i \dot{V}_i \Delta T_i', \qquad (17)$$

where $\Delta T_i' = \Delta T_i / \Delta T$. Equation 17 is similar in form to equation 15; however, in this case there is no relationship between ΔT and the sum of the ΔT_i, so that $\dot{V}$ is not the weighted mean of the component flows as before. Nevertheless, if all of the flow rates in the original system are doubled with temperatures remaining as they were originally, the flow $\dot{V}$ will also double, since each of the $\dot{V}_i$ in equation 17 will double with the ΔT_i remaining constant. In a sense, then, the replacement flow $\dot{V}$ is a measure of the over-all flow to the system; its magnitude is responsive to a simultaneous change in magnitude of all of the component flows. Similarly, changing any single $\dot{V}_i$ in equation 17 will also change the magnitude of $\dot{V}$ if $\Delta \dot{V}_i$ is not zero. To express this in general terms, the single flow model depends only on the assumption that any change in blood flow to the nasal regions is uniformly distributed throughout the vascular bed.

Components of the Model

Fig. 2 shows a diagram of the nasal passage, including the liquid (blood) flow stream depicted in Fig. 1. The dotted line indicates a boundary which encloses the nasal passages and mucosa, beginning at a given distance from the tip (boundary *X*), extending along boundary *Y*, to a depth where the temperature equals body core temperature (boundary *Z*). Energy transported across this boundary can be separated conceptually into four components: (*a*) the change in internal energy of water entering across boundary *Y* in liquid form from the body core and leaving as expired vapor (that fraction of the water which is evaporated into the airstream during inspiration and recondensed during expiration does not enter into the net energy transport across the boundary); (*b*) the change in internal energy of the respired air; (*c*) the thermal conduction to or from the environment through the nose tip; and (*d*) the change in internal energy of blood flowing to the area, including thermal conduction from the body core through the tissues to the area. Because mixtures of air and water vapor behave approximately as ideal gases at physiological temperature and pressure, their enthalpies[1] are additive, making it possible to deal separately with changes in enthalpy within the boundary for each of the four components.

Energy Transfer to Expired Vapor Entering as Liquid. Blood supplies both heat and water to the nasal mucosa. Part of the water is evaporated during inspiration and is not recondensed during expiration, leaving the boundary as vapor and thus undergoing a substantial increase in enthalpy within the boundary. In Fig. 2,

[1] In respiratory exchange, changes in enthalpy and internal energy are approximately equal.

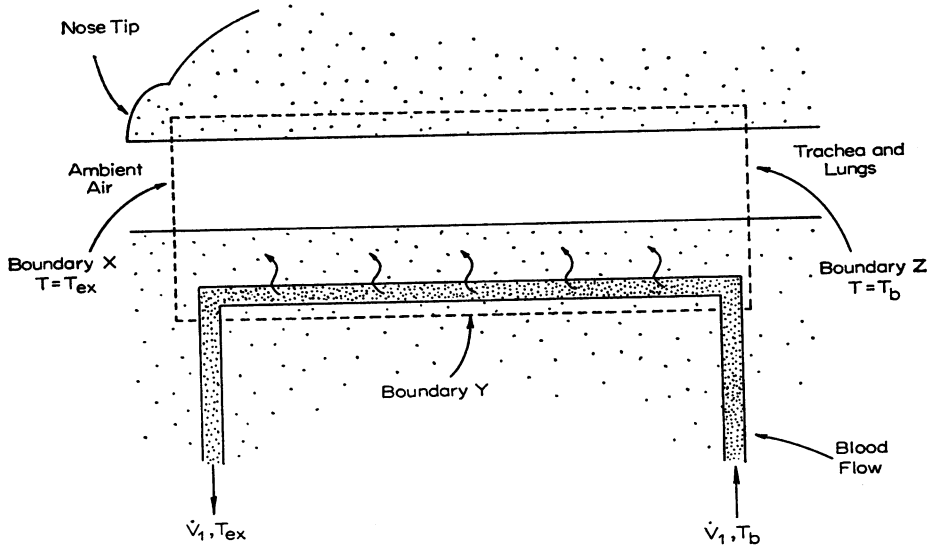

FIGURE 2 Diagram of nasal passage region of kangaroo rat. Dotted lines denote boundary of system for which energy balance is considered.

boundary X is at the minimum depth (1 mm) where observed cyclical fluctuations in airstream temperature were consistently small (0.3°C or less), indicating that inspired air has reached approximate wall temperature at this depth.

Inspired air would also be approximately saturated with water vapor at X if sufficient water were available on the passage wall exterior to that depth; however, both direct observation of the animals and experiments indicate that there is no substantial evaporation from the first 1 mm of the passage.[2] It is therefore reasonable to assume that inspired and expired air cross boundary X of Fig. 2 at approximately the same temperature (T_{ex}), that inspired air crosses boundary X at approximately ambient absolute humidity, and that expired air crosses boundary X saturated with water vapor.

The rate of respiratory water loss is the product of air flow rate (ventilation rate) and the difference in absolute humidity of ambient air and expired air. If it is assumed that all the water lost in this way originally entered the bounded area in liquid form at body core temperature T_b, the rate of heat transfer to this component

[2] Examination of the nose tip indicates that its inner surface is poorly suited for evaporation. The surface is not well supplied with blood, unlike the richly perfused mucosa at greater depth, and is covered with a thin layer of dried mucus which seems to originate from greater depth.

To determine the effect of interrupting evaporation, nasal passage temperature profiles (temperature as a function of passage depth) were obtained from an animal before and after a layer of collodion was spread over the nasal surfaces. Coating substantial areas of the deeper surfaces caused significant changes in the profiles, indicating that the collodion did inhibit evaporation significantly; however, coating only the nose tip did not substantially alter the profiles, suggesting negligible evaporation from the nose tip surfaces.

of expired vapor is

$$\dot{V}_a([W]_{ex} - [W]_a)(H_{v,\,ex} - H_{w,\,b}). \tag{18}$$

$\dot{V}_a$ is ventilation rate in grams dry air per second; $([W]_{ex} - [W]_a)$ is the difference in absolute humidities of air saturated at T_{ex} and ambient air; and $H_{v,ex}$ is the enthalpy of water vapor at T_{ex}, and $H_{w,\,b}$ that of water at T_b, both in calories·gram^{-1}.

If the reference level of enthalpy is taken to be that of liquid water at 0°C, the enthalpy of the water lost by evaporation is numerically equal to temperature T_b when it enters at boundary Y, and equal to $(596.88 + 0.444\,T_{ex})$ when it leaves at boundary X (Zimmerman and Lavine, 1945). If these numerical values are introduced into equation 18, we obtain for the energy transfer to expired vapor entering as liquid

$$\dot{V}_a([W]_{ex} - [W]_a)(596.88 + 0.444T_{ex} - T_b). \tag{19}$$

Energy Transfer to the Remainder of the Respired Air. During inspiration air crosses boundary Z (Fig. 2) saturated with water vapor at approximately body core temperature, and during expiration reenters at boundary Z under approximately the same conditions. In the lungs, there is a nominal 5% volumetric exchange of oxygen for carbon dioxide. If a nominal temperature differential between boundary X and boundary Z of 15°C is also assumed, then the energy extracted during expiration from the carbon dioxide differs from that added during inspiration to the oxygen by about 0.04 cal g^{-1} respired air, which is about 1% of the increase in energy of expired vapor supplied by the mucosa and is therefore negligible.

The energy added during inspiration to the components of respired air (including inspired vapor, inspired dry air, and water evaporated into the airstream during inspiration and recondensed during expiration) is extracted from these components during expiration (air enters and leaves at boundary X at the same temperature). Thus, there is no net change in the enthalpy of respired air (excluding expired vapor supplied by the mucosa) within the boundary of Fig. 2.

Energy Transfer through the Nose Tip. This transfer occurs through the tissues and through the surrounding boundary layer of air. The rate of thermal conduction through the combined system (i.e., across boundary X) can be estimated by making simplifying assumptions about its geometry and characteristics. As an approximation assume the nose tip to be a hemisphere with outer radius 1.5 mm (about that of the nose tip) and thickness 1 mm, with the inner surface maintained at temperature T_{ex}. If a value of 9.8×10^{-4} cal (cm °C sec)$^{-1}$ is used for the thermal conductivity of the nasal tissue (Davis, 1963), the thermal resistance for the hemisphere can be estimated to be 2.16×10^3 sec °C cal^{-1} assuming spherical symmetry for thermal conduction (Schenck, 1959; Eckert and Gross, 1963).

The layer of air surrounding the nose tip was explored with a self-heated thermistor

which was adjusted to respond well at the air velocity of transition from free to forced convection (about 20 cm/sec for the geometry of the nose tip) (Kreith, 1965). No cyclical cooling was observed at any location, except directly in front of the nasal orifices, indicating that the nose tip outer surface is cooled by free (as opposed to forced) convection. Under this assumption, we estimate a thermal resistance for the boundary layer of air of 1.77×10^4 sec °C cal^{-1}. The total thermal resistance[3] will be the sum of the two components, or 1.98×10^4 sec °C cal^{-1}. When inverted this yields a rate of total heat loss by thermal conduction through the nose tip of

$$5.05 \times 10^{-5}(T_{ex} - T_a) \text{ cal sec}^{-1}. \quad (20)$$

Energy Transfer from Blood and from the Body Core. Blood flowing to the nasal region (excluding the expired vapor supplied by the mucosa, which originates in the bloodstream) undergoes a decrease in enthalpy within the boundary of Fig. 2. It is not feasible to determine directly the rate and distribution of this blood flow and thus the rate of energy transfer from the blood; however, the blood flow may be replaced conceptually by an equivalent liquid stream entering the system at temperature T_b (boundary Z), flowing inside the system parallel to boundary Y, and leaving the system at temperature T_{ex} (boundary X). If a specific heat equal to that of water (1 cal g^{-1} °C^{-1}) is assigned to the liquid[4] (of flow rate $\dot{V}_l$), the rate of energy transfer from this component within the system can be expressed as:

$$\dot{V}_l(T_b - T_{ex}). \quad (21)$$

Thermal conduction through the tissue from the body core across the boundary of Fig. 2 can be included in the heat transferred from the liquid stream. The effective stream flow rate is therefore a composite of blood flow and of thermal conduction from the body core.

Energy Balance Equation

Of the four components of energy transfer discussed above, item *b* was found to be negligible, and items *a*, *c*, and *d* can now be combined to give the following energy balance equation:

$$\dot{V}_a([W]_{ex} - [W]_a)(596.88 + 0.444T_{ex} - T_b) + 5.05 \times 10^{-5}(T_{ex} - T_a) = \dot{V}_l(T_b - T_{ex}). \quad (22)$$

---

[3] According to these calculations 89% of the total temperature difference between T_{ex} and T_a should reside in the boundary layer of air. 29 measurements on five animals yielded an average of 75% and a standard deviation of 68%. This large standard deviation is not surprising since many of the temperature differences encountered were less than 1°C.

[4] The exact value of specific heat is not important since it appears only as a constant of proportionality.

All parameters in this equation except $\dot{V}_l$ can be either measured directly or estimated from physiological measurements, and it is therefore possible to calculate the liquid stream flow $\dot{V}_l$ for any animal under given ambient conditions. This will be done below, yielding equation 28, which is then used in producing the final desired model as given by equations 30 *a* and 30 *b*.

PHYSIOLOGICAL MEASUREMENTS

The physiological variables to be used in equation 22 are body core temperature T_b, exhaled air temperature T_{ex}, and ventilation rate $\dot{V}_a$. The latter cannot be measured readily in the living animal, but can be estimated with reasonable accuracy from the oxygen consumption rate. The effective flow rate of the liquid stream $\dot{V}_l$ is a model parameter which will be estimated from the preceding variables.

Rectal Temperature

The animals were restrained in a near-natural position. A rubber-covered U-shaped clamp behind the head prevented movements of the head without exerting undue pressure. Rectal temperature, measured with a thermistor probe, was found to vary regularly with ambient temperature (Fig. 3). The least-squares regression line for these data gives

$$T_b = 29.4 + 0.327T_a . \tag{23}$$

These data vary more with ambient temperature than previously reported values (Schmidt-Nielsen, 1964), probably because they were obtained from restrained animals.

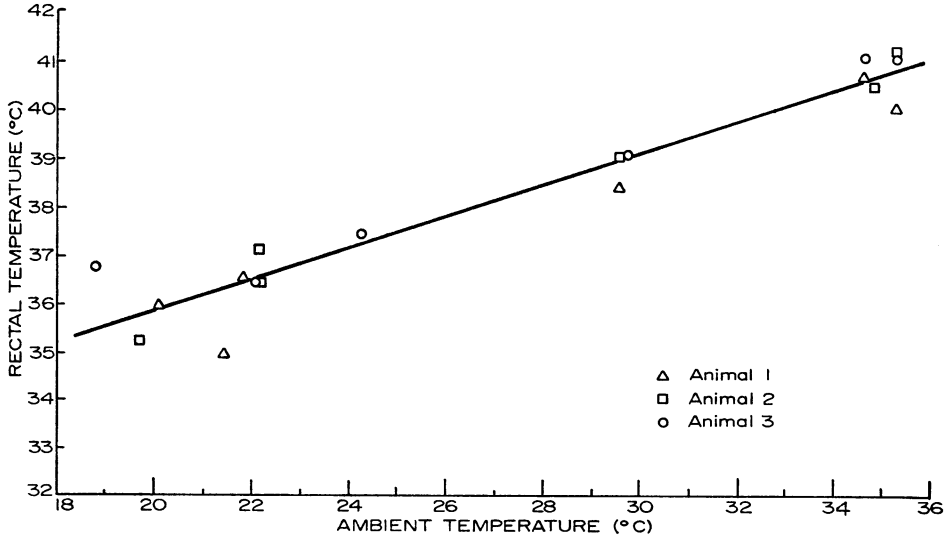

FIGURE 3 Body temperature of kangaroo rat as a function of ambient air temperature. The solid line is the linear regression of body temperature on ambient temperature.

Nasal Temperatures

The animals were restrained as above and nasal temperatures measured with a microbead thermistor probe whose basic features have been described previously (Schmidt-Nielsen et al., 1970).

The probe was inserted as far as possible (about 25 mm) and was then retracted in 1 mm steps with nasal temperature recorded at each step and at positions on the nose tip surface after retraction. The range of ambient temperature used for any particular animal was that over which the restrained animal would maintain nearly constant rectal temperature during the measurements.

Figs. 4 and 5 display typical nasal temperature profiles. In Fig. 4, profiles obtained from two different animals under approximately the same ambient conditions are shown. The profiles in Fig. 5 were obtained from a single animal at approximately constant environmental temperature and illustrate the effect of humidity on nasal passage temperatures.

Measurements of ambient temperature and humidity, rectal temperature, nose tip temperature, and nasal temperature at the maximum depth obtained at a variety of ambient conditions on these animals are given in Table I. It is remarkable that nose tip temperatures could be as much as 10°C below ambient temperature.

Rate of Oxygen Consumption

The rate of oxygen consumption was determined on the same animals as used for temperature measurements, but in separate experiments covering the same temperature range. The pro-

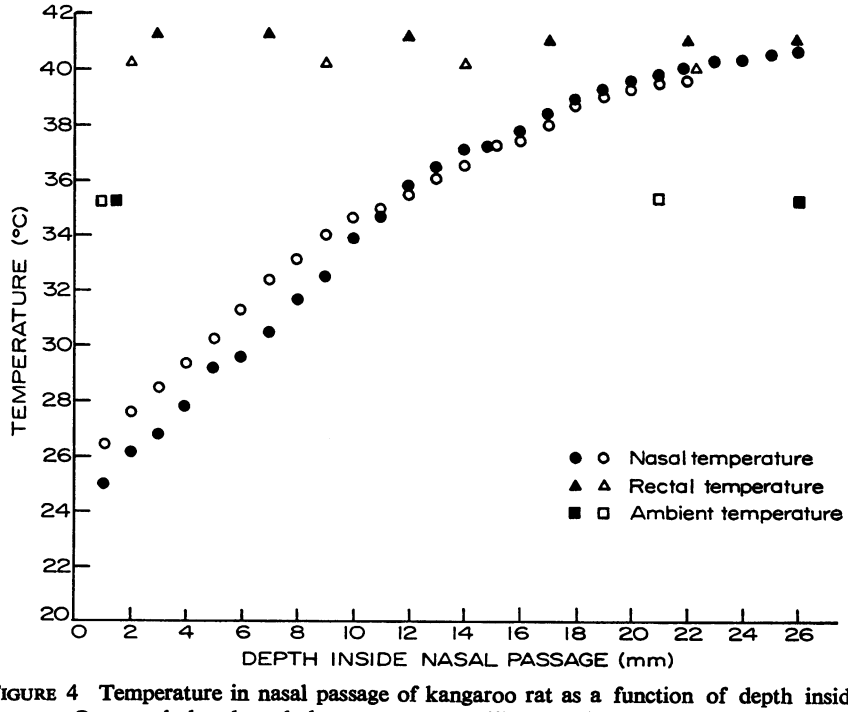

FIGURE 4 Temperature in nasal passage of kangaroo rat as a function of depth inside passage. Open and closed symbols represent two different animals. Open symbol relative humidity is 28.5%; closed symbol is 27.5%.

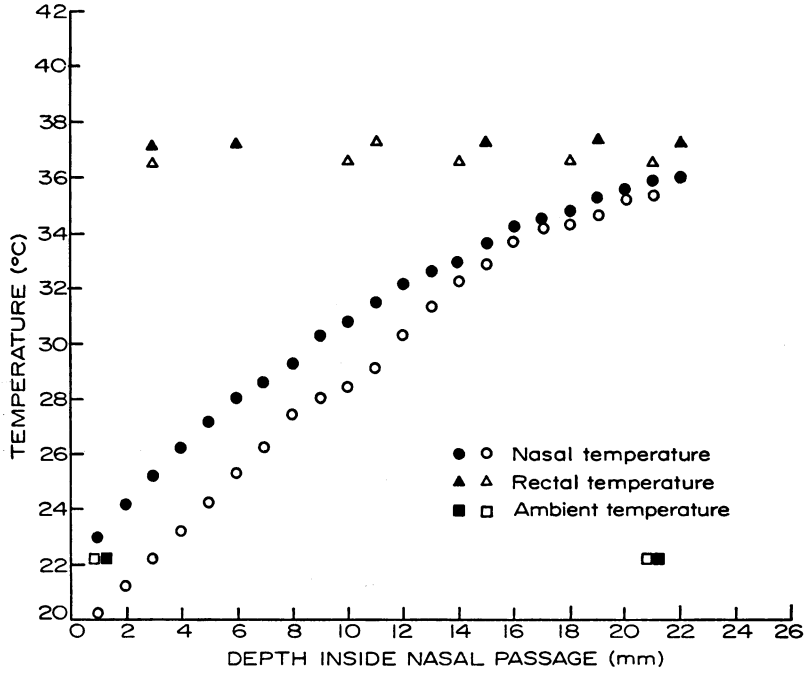

FIGURE 5 Temperature in nasal passage of kangaroo rat as a function of depth inside passage. Open symbols represent 37% relative humidity and closed symbols, 62.5%.

cedures were standard, determining the decrease in oxygen concentration as air was passed through an animal chamber (Depocas and Hart, 1957). The airstream was adjusted to keep the CO_2 concentration in the chamber below 0.3%. No correction was made for the change in volume of respiratory air due to replacement of inspired O_2 by expired CO_2 ; the CO_2:O_2 ratio (RQ) was considered to equal unity because the animals were on a predominately carbohydrate diet (grain).

As a matter of convenience in later computations the rates of oxygen consumption are expressed as milliliters oxygen at body temperature (37°C), ambient pressure, and saturated with water vapor (BTPS). The values are normalized by being expressed per 100 g body weight (which is close to the actual body weight of these kangaroo rats, around 90 g).

Rates of oxygen consumption of three animals at various ambient conditions are given in Table II. The variation in the rate with temperature is similar to previously reported data (Carpenter, 1966).

Estimated Tidal Volume and Ventilation Rates

The ventilation rate $\dot{V}_a$, which is needed for the solution of equation 22, can be estimated from the oxygen consumption rate $\dot{V}_{O_2}$, but only if the relative role of the respiratory dead space is known. It is also necessary to know the respiratory frequency f_{resp} . Then with information about environmental, alveolar, and dead space oxygen concentrations $\dot{V}_a$ can be calculated.

The tidal volume V_T is the sum of the physiological dead space V_D and the alveolar ex-

TABLE I

NASAL AND RECTAL TEMPERATURES MEASURED ON THREE KANGAROO RATS*

T_a Ambient temp	Ambient relative humidity	T_{ex} Nose tip (1 mm) temp	T_b Rectal temp	Deep nasal temp	Maximum depth
°C	%	°C	°C	°C	mm
20.05	30	17.6	36.0	35.4	22
21.45	37	19.0	25.0	34.0	25
21.85	56	23.2	36.6	36.3	22
29.55	28.5	25.6	38.5	38.35	25
34.6	60	31.4	40.8	40.25	25
35.3	16	26.5	40.2	39.6	22
19.7	30	17.5	35.3	35.0	22
22.15	62.5	23.0	37.2	36.0	22
22.2	37	20.3	36.5	35.3	21
29.55	28	24.0	39.1	38.0	22
34.85	61	31.85	40.6	40.35	20
35.3	19	25.3	41.3	40.8	21
18.8	61	21.2	36.8	36.1	21
22.1	50	22.9	36.5	36.85	20
24.25	33	22.7	37.5	37.15	23
29.55	27.5	25.0	39.1	39.2	24
34.6	56	31.0	41.2	40.3	24
35.3	17	25.0	41.2	40.7	26

* Data used to obtain equations 30 *a* and 30 *b* from equation 22.

change volume V_A . V_A may be expressed as

$$V_A = \frac{\dot{V}_{O_2}}{f_{resp}([O_2]_{\bar{L}} - [O_2]_D)}, \tag{24}$$

where $[O_2]_D$ is the mean oxygen concentration of air in the dead space at the beginning of inspiration and $[O_2]_{\bar{L}}$ is the concentration of air entering the alveoli. $[O_2]_{\bar{L}}$ may be expressed as

$$[O_2]_{\bar{L}} = [O_2]_a - \frac{V_D}{V_T}([O_2]_a - [O_2]_D), \tag{25}$$

where $[O_2]_a$ is the oxygen concentration of ambient air.

If equation 25 is substituted into equation 24 and V_D is added to the result, the sum is a quadratic expression in which V_T has the solution

$$V_T = V_D + \frac{\dot{V}_{O_2}}{2f_{resp}([O_2]_a - [O_2]_D)} + \sqrt{\frac{4V_D\dot{V}_{O_2}f_{resp}([O_2]_a - [O_2]_D) + (\dot{V}_{O_2})^2}{4\{f_{resp}([O_2]_a - [O_2]_D)\}^2}}. \tag{26}$$

TABLE II

COMPREHENSIVE TABULATION OF RESPIRATORY VARIABLES NORMALIZED TO 100 g BODY WEIGHT*

Ambient temp	Respiration rate	Mean O_2 in chamber	O_2 consumption	Tidal vol	Ventilation rate
°C	sec^{-1}	%	$[BTPS\ cm^3\ (g\ sec)^{-1}] \times 10^{-4}$	$BTPS\ cm^3$	$[BTPS\ cm^3\ sec^{-1}] \times 10^{-3}$
21.8	1.27	20.58	4.89	1.037	1.32
22.2	1.10	20.67	3.63	0.953	1.04
27.5	0.82	20.73	2.83	0.971	0.80
28.1	1.25	20.68	3.53	0.880	1.10
34.0	0.98	20.79	2.01	0.757	0.74
34.0	1.05	20.78	2.17	0.757	0.95
21.5	1.13	20.68	4.43	1.032	1.17
22.3	1.05	20.72	3.74	0.978	1.03
27.4	0.84	20.76	3.00	0.979	0.82
27.9	1.15	20.76	2.96	0.835	0.95
34.0	1.02	20.80	2.23	0.771	0.79
34.0	1.10	20.79	2.51	0.785	0.86
22.2	1.00	20.60	4.59	1.125	1.13
22.8	1.00	20.61	4.72	1.161	1.15
27.4	1.18	20.68	3.69	0.923	1.08
28.4	1.12	20.68	3.63	0.941	1.04
34.0	1.21	20.74	2.74	0.785	0.94
34.2	1.14	20.77	2.43	0.770	0.87

* Data used to obtain equations 30 *a* and 30 *b* from equation 22.

Alveolar oxygen concentration $[O_2]_A$, assumed to be equal to $[O_2]_D$, is difficult to determine for the kangaroo rat because of its small size; however, information about the oxygen dissociation curve of the blood and the arterial carbon dioxide levels in the kangaroo rat (Gjönnes and Schmidt-Nielsen, 1952) indicates that lung and blood gas exchange is similar to that of mammals in general, and we will use $[O_2]_A$ as equal to that in man, or about 13.1% of a standard atmosphere (Rahn, 1954).

The anatomical dead space is also difficult to determine in kangaroo rats because the injection of cast material causes considerable distension of the thin-walled bronchioles. We therefore estimate the functional dead space V_D from the expression $V_D = 2.76$ (body weight in kilograms)$^{0.96}$ (Stahl, 1967).

Values of the $\dot{V}_{O_2}$, f_{resp}, and $[O_2]_a$ were determined experimentally (Table II). Estimates of V_T obtained from equation 26 multiplied by respiratory frequency f_{resp}, give corresponding values of ventilation rate $\dot{V}_a$ (also tabulated in Table II).

The ventilation rates obtained at low, moderate, and high ambient temperatures for a given animal were averaged for each of the three temperatures. It was then assumed that ventilation rates at temperatures below the moderate ambient temperature (about 28°C) were on a straight line determined by the mean low- and moderate-temperature ventilation rates, and that rates for above-moderate temperatures were on a similar line determined by the mean

TABLE III

EXPERIMENTALLY DETERMINED VALUES OF TERMS IN ENERGY BALANCE EQUATION NORMALIZED TO 100 g BODY WEIGHT*

T_a Ambient conditions		T_b T_{ex} Temperatures		$\dot{V}_a$ Estimated ventilation rate	$\dot{V}_l$ Stream flow rate	Rate of respiratory energy loss	Rate of respiratory water loss	Efficiency of vapor recovery (dimensionless)
Temp	Relative humidity	Body	Nose tip					
°C	%	°C	°C	[g dry air sec^{-1}] $\times 10^{-3}$	[g liquid sec^{-1}] $\times 10^{-4}$	[cal sec^{-1}] $\times 10^{-3}$	[g sec^{-1}] $\times 10^{-5}$	
20.05	30	36.0	17.6	1.34	3.16	5.81	1.04	0.773
21.45	37	35.0	19.0	1.28	3.53	5.67	1.01	0.745
21.85	56	36.6	23.2	1.27	4.76	6.39	1.10	0.718
29.55	28.5	38.5	25.6	0.96	5.52	7.11	1.28	0.643
34.6	60	40.8	31.4	0.80	3.84	3.61	0.65	0.726
35.3	16	40.2	26.5	0.78	4.94	6.78	1.26	0.630
19.7	30	35.3	17.5	1.26	3.35	5.97	1.04	0.750
22.15	62.5	37.2	23.0	1.16	3.41	4.83	0.84	0.765
22.2	37	36.5	20.3	1.16	3.52	5.72	1.02	0.741
29.55	28	39.1	24.0	0.93	3.83	5.78	1.07	0.706
34.85	61	40.6	31.85	0.87	4.52	3.94	0.72	0.710
35.3	19	41.3	25.3	0.86	3.76	6.00	1.15	0.708
18.8	61	36.8	21.2	1.27	3.58	5.58	0.96	0.766
22.1	50	36.5	22.9	1.22	4.77	6.50	1.13	0.706
24.25	33	37.5	22.7	1.19	5.05	7.47	1.32	0.691
29.55	27.5	39.1	25.0	1.09	5.50	7.75	1.40	0.673
34.6	56	41.2	31.0	0.95	4.58	4.67	0.85	0.725
35.3	17	41.2	25.0	0.93	4.23	6.86	1.29	0.702

* Data used to obtain equations 30 *a* and 30 *b* from equation 22.

moderate- and high-temperature rates. Ventilation rates for ambient conditions corresponding to those for which nasal and rectal temperatures were measured were estimated in this way (see Table III, fifth column).

EVALUATION AND UTILIZATION OF THE MODEL

Use of Experimental Data for Substitution in Energy Balance Equation

Table III contains values for variables in the energy balance equation for every set of ambient conditions under which nasal and rectal temperatures were measured, as well as some physiologically relevant combinations of these variables, including the efficiency of vapor recovery during expiration. Values of net rate of respiratory energy transfer and of rate of respiratory water loss are approximately the same for the three animals at similar ambient conditions, although the values for the second animal are generally lower, and those for the third animal, higher, than those for

the first animal. Both rates are considerably lower for hot, humid environments than for other conditions.

The efficiency of respiratory vapor recovery can be defined as the ratio of the amount of water recondensed on the passage walls during expiration to that evaporated from the walls during inspiration, or

$$\text{Efficiency of vapor recovery} = ([W]_b - [W]_{ex})/([W]_b - [W]_a). \quad (27)$$

The efficiency of vapor recovery depends on the passage geometry (smaller transverse dimensions and greater axial length improve efficiency), and also on the rates of blood flow and respiratory air flow. The calculated efficiencies in Table III are all between 63 and 77%. Fig. 6 shows the liquid stream flow rate, $\dot{V}_l$, normalized to 100 g body weight and plotted as a function of T_{ex}. It appears to decrease systematically with T_{ex}. The relative decrease in Fig. 6 is much less than the vasoconstrictive decreases in blood flow observed in extremities (Thauer, 1964); nevertheless, the decrease is statistically significant. The least-squares linear regression of $\dot{V}_l$ on T_{ex} is

$$\dot{V}_l = 2.21 \times 10^{-4} + 8.33 \times 10^{-6} T_{ex} \text{ g(100 g body wt)}^{-1} \text{ (sec)}^{-1}. \quad (28)$$

The regression slope differs from zero by about twice its standard deviation and about three times its probable error, if independent, normally distributed errors are assumed (Merriman, 1911).

The mean ventilation rates, $\dot{V}_a$, estimated for each animal were normalized to 100 g body weight and averaged for each of three temperatures, giving three over-all

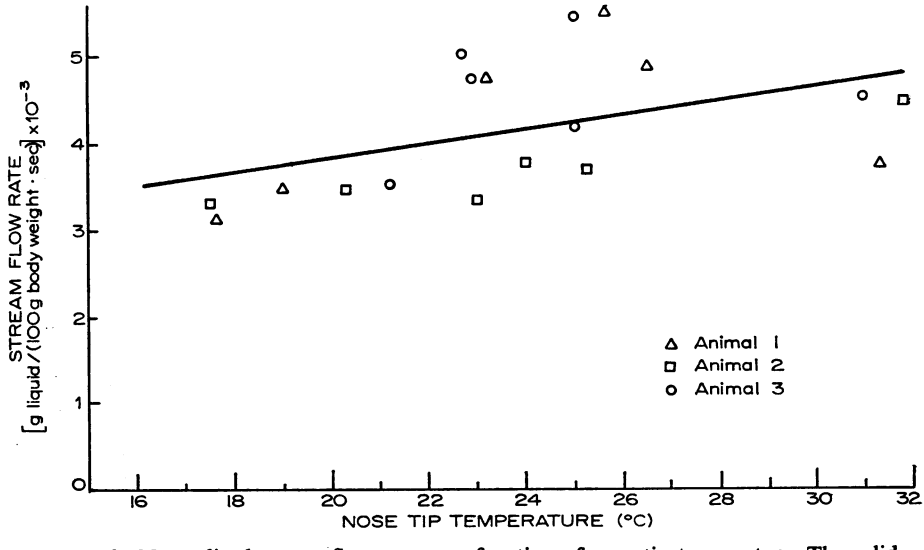

FIGURE 6 Normalized stream flow rate as a function of nose tip temperature. The solid line is the linear regression of stream flow rate on nose tip temperature.

ventilation rates. These rates were assumed to define a piecewise linear function of ventilation rate and ambient temperature,

$$\dot{V}_a(T_a \leq 27.8°\text{C}) = 1.94 \times 10^{-3} - 3.25 \times 10^{-5} T_a \text{ g dry air (100 g body wt)}^{-1} \text{ (sec)}^{-1}; \quad (29\,a)$$

$$\dot{V}_a(T_a > 27.8°\text{C}) = 1.67 \times 10^{-3} - 2.30 \times 10^{-5} T_a \text{ g dry air (100 g body wt)}^{-1} \text{ (sec)}^{-1}. \quad (29\,b)$$

We can now insert equations 23, 28, and 29 *a* or 29 *b* into equation 22. The result is an *energy balance equation which expresses expired air temperature and humidity in terms of ambient temperature and humidity*, with all other variables eliminated from the expression.

$$(1.10 - 1.91 \times 10^{-2} T_a + 8.61 \times 10^{-4} T_{ex} - 1.06 \times 10^{-5} T_a^2 + 1.42 \times 10^{-5} T_a T_{ex})([W]_{ex} - [W]_a) - 1.225 \times 10^{-4} T_a + 2.64 \times 10^{-5} T_{ex} - 2.72 \times 10^{-6} T_a T_{ex} + 8.33 \times 10^{-6} T_{ex}^2 - 6.49 \times 10^{-3} = 0 \quad (\text{for } T_a \leq 27.8°\text{C}); \quad (30\,a)$$

$$(0.948 - 1.358 \times 10^{-3} T_a + 7.42 \times 10^{-4} T_{ex} - 7.50 \times 10^{-6} T_a^2 - 1.019 \times 10^{-5} T_a T_{ex})([W]_{ex} - [W]_a) - 1.225 \times 10^{-4} T_a + 2.64 \times 10^{-5} T_{ex} - 2.72 \times 10^{-6} T_a T_{ex} + 8.33 \times 10^{-6} T_{ex} - 6.49 \times 10^{-3} = 0 \quad (\text{for } T_a > 27.8°\text{C}). \quad (30\,b)$$

We now have eliminated from the original model, equation 22, those physiological variables which are not readily measured. By substituting generalized expressions for these, we have the means to predict, from measured ambient air temperature and humidity, the expired air temperature and humidity.

Equations 30 *a* and 30 *b* not only specify expired air temperature and humidity for given ambient conditions, but also imply numerical values of physiological quantities including (*a*) rate of respiratory energy loss, (*b*) rate of respiratory water loss, and (*c*) efficiency of vapor recovery as functions of ambient conditions.

Internal Consistency of Model as Compared to Experimental Data

To test whether the model is internally consistent with the physiological measurements used to derive its numerical parameters, model calculations are compared with the physiological data. In this discussion "calculated" means calculated by the generalized model (equations 30 *a* and 30 *b*), while "observed" refers to values

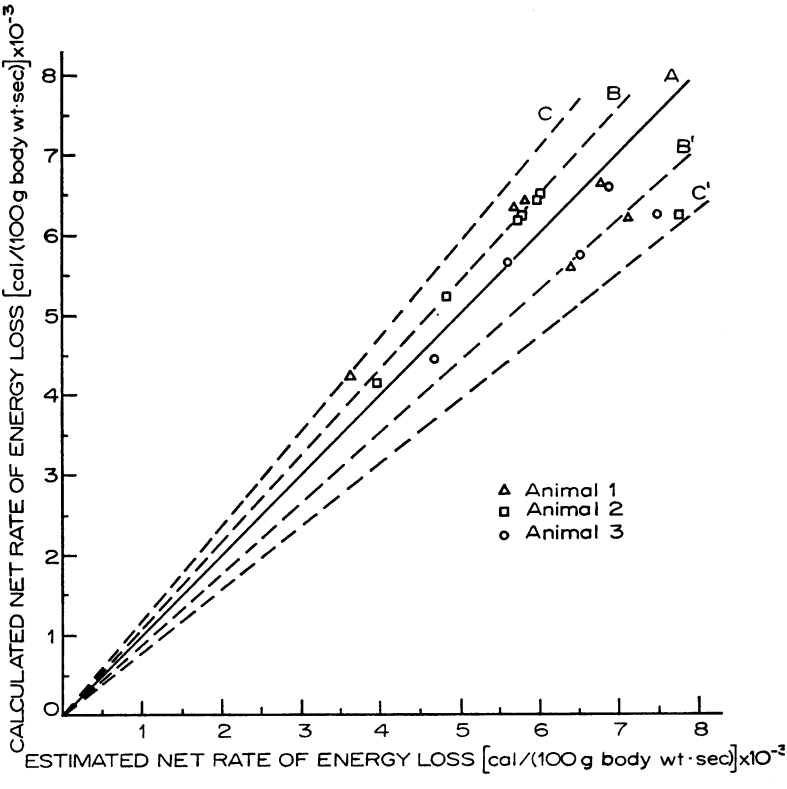

FIGURE 7 Calculated net rate of respiratory energy loss vs. estimated values based on physiological measurements and assumptions, normalized to 100 g body weight. Line A, calculated loss = estimated loss; lines B, B′ represent ±10%; lines C, C′ represent ±20%.

estimated from physiological measurement on the three previously mentioned kangaroo rats. Calculated and observed values of the rate of respiratory energy loss are plotted in Fig. 7. Every rate calculated by equations 30 *a* and 30 *b* is within 20% of the corresponding observed rate, the mean percentage error in predicted rates is 1.5%, and the standard deviation of error is ±11%. Thus the equations calculate energy transfer rates for the three animals with a standard deviation of 11%.

Calculated and observed values of the rate of respiratory water loss are plotted in Fig. 8. The pattern is very similar to that in Fig. 7. All calculated rates agree to within 20% of the corresponding observed values, the mean percentage error in predicted rates is 1.6%, and the standard deviation is ±10.4%. Again, the equations calculate respiratory water loss rate for the three animals with a standard deviation of about 11%.

Calculated and observed values of the efficiency of respiratory vapor recovery (equation 27) are plotted in Fig. 9. Calculations are within 0.05 of the corresponding observed values, the mean error is 0.014, and the standard deviation of error is

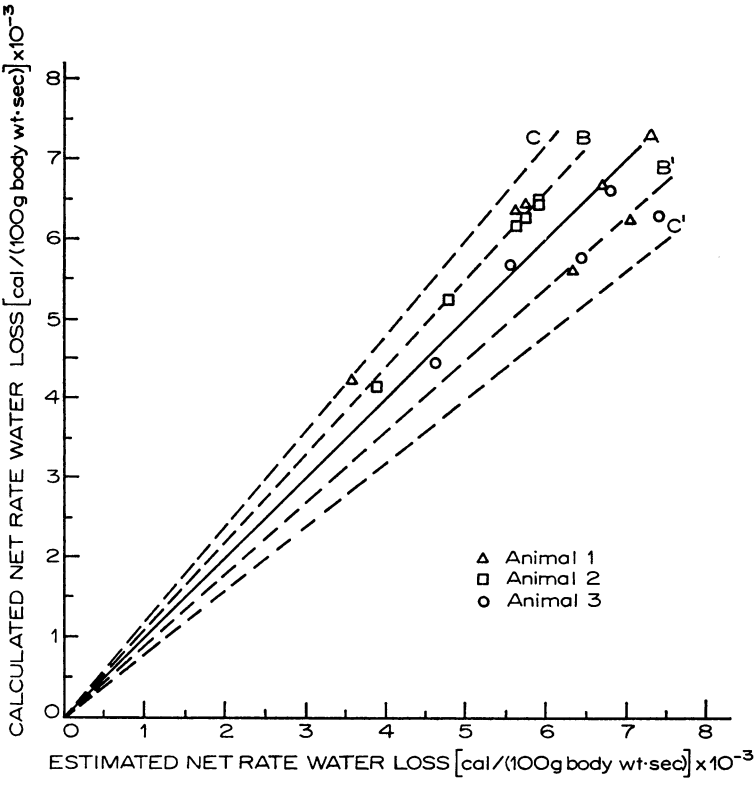

FIGURE 8 Calculated values of net rate of respiratory water loss vs. estimated values based on physiological measurements and assumptions, normalized to 100 g body weight. Line A, calculated loss = estimated loss; lines B, B′ represent ±10%; lines C, C′ represent ±20%.

±0.030. In every case, observed values of efficiency are between 0.63 and 0.77 and calculated values are between 0.66 and 0.74.

Conservation of heat and water in the nasal passages is in many respects analogous to that in the heat regenerator of a Stirling engine. Theoretical and experimental analyses of Stirling regenerators involving only thermal diffusion have yielded enthalpy recovery efficiencies of greater than 0.95 (Qvale and Smith, 1969); however, in the kangaroo rat, blood flow to the nasal area warms the passages and thus lowers the over-all efficiency of vapor recovery.

The difference between expired air temperature T_{ex} and ambient air temperature T_a is particularly interesting. For conditions under which T_{ex} is less than T_a, it is obvious that evaporative cooling (mass transfer) must be taking place. The differences in calculated and measured values of this quantity indicate how accurately the energy balance equations will calculate T_{ex} when T_a is known. Calculated and measured values of $(T_{ex} - T_a)$ are shown in Fig. 10. The mean error in calculated

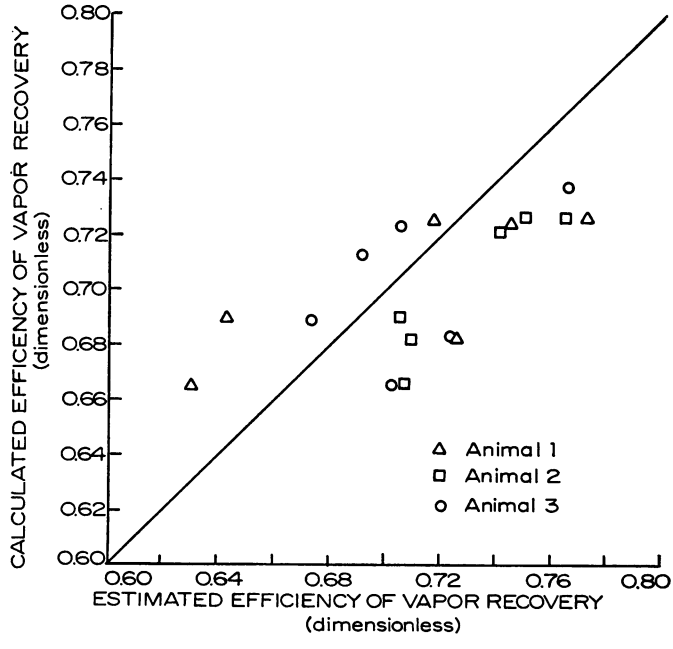

FIGURE 9 Calculated values of efficiency of vapor recovery in the nasal passages vs. values estimated from physiological measurements and assumptions.

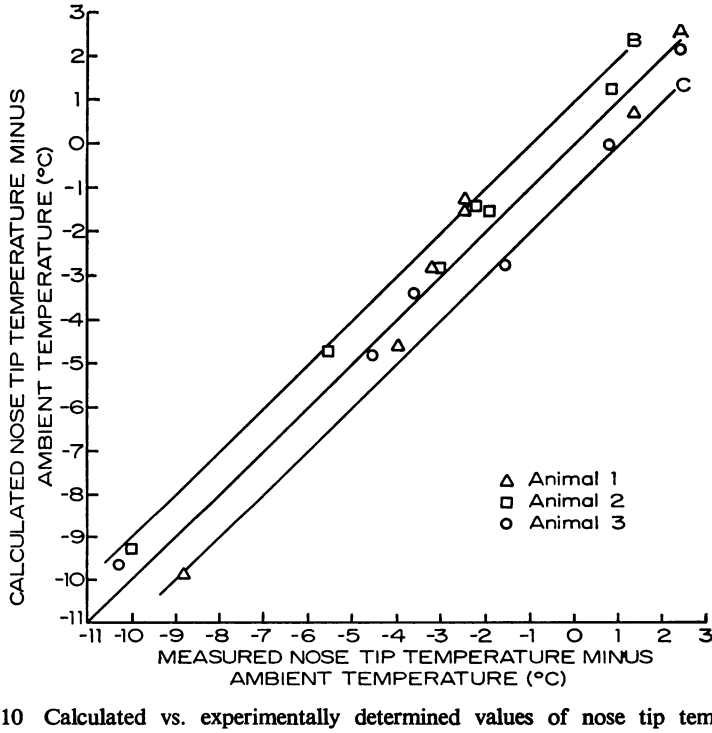

FIGURE 10 Calculated vs. experimentally determined values of nose tip temperature minus ambient temperature. Line A, calculated nose tip temperature = measured nose tip temperature; lines B and C represent ±1.0° C deviation.

T_{ex} is 0.125°C, the standard deviation of error is ±0.73°C, and all calculated T_{ex} are within 1.2°C of the measured T_{ex}.

In conclusion, the internal consistency of the model is described by the preceding comparison of the model with the data from which it was derived. The observed errors are considered to be within acceptable limits for consistency.

TABLE IV

COMPARISON OF MODEL-PREDICTED EXPIRED AIR TEMPERATURES WITH THOSE MEASURED ON EIGHT KANGAROO RATS

Ambient conditions		Expired air temperature		
Temp	Relative humidity	Predicted	Measured	Error
°C	%	°C	°C	°C
18.65	62	21.0	19.5	1.5
23.5	49	22.9	23.7	−0.8
18.6	63	21.1	20.95	0.15
18.65	62	21.0	20.45	0.55
21.45	40	20.6	22.5	−1.9
23.4	48	22.8	22.8	0
29.55	32	24.7	27.9	−3.2
35.1	56	31.6	32.3	−0.7
18.85	61	21.1	21.0	0.1
22.15	48	21.9	22.5	−0.6
24.25	31	21.3	20.5	0.8
29.6	27	24.0	23.85	0.15
34.6	56	31.3	31.6	−0.3
35.3	18	25.8	24.75	1.05
19.2	57	20.9	20.3	0.6
24.5	38	22.3	22.1	0.2
28.5	32	24.1	25.0	−0.9
19.3	57	21.0	19.8	1.2
24.5	38	22.3	22.5	−0.2
28.5	32	24.1	25.4	−1.3
19.3	58	21.1	19.0	2.1
24.6	39	22.5	23.5	−1.0
28.6	33	24.3	24.5	−0.2
19.4	58	21.1	20.6	0.5
24.6	40	22.6	23.1	−0.5
28.7	34	24.5	24.7	−0.2
19.4	58	21.1	21.0	0.1
24.7	40	22.7	22.6	0.1
28.9	37	25.0	25.2	−0.2

Predictive Value of Model: Comparison to Additional Physiological Measurements

In order to check the predictive value of the model, expired air temperatures were measured on eight additional animals at various ambient conditions. Table IV compares observed values with values predicted by equation 30 *a* and 30 *b*. The mean error in predicted expired air temperatures for these animals is −0.1°C and the standard deviation is ±1.04°C. 18 of the 29 errors are within one standard deviation of the model-temperature-error mean (0.125°C), and 26 are within two model-error standard deviations. If the samples were obtained from identical normally distributed populations, 20 and 28 errors, respectively, would be expected to be within these ranges. Thus, the predicted expired air temperatures appear to fit the measured nasal temperatures to within a standard deviation of 1°C.

A certain amount of correlation is to be expected between the errors in predicted expired air temperature and in other predicted quantities. For example, expired air temperature predictions that are too low would generally be accompanied by too low predictions of respiratory energy loss and water loss rates and too high predictions of efficiency of vapor recovery. For the data of Figs. 7–10, the correlation coefficient of expired air temperature error and energy loss rate error is 0.78, that of expired air temperature error and water loss rate error is 0.72, and that of expired air temperature error and efficiency of vapor recovery error is −0.83. Errors in predictions of these additional respiratory quantities are, therefore, highly correlated with expired air temperature errors.

Use of Model: Generalized Predictions

The energy balance model (equation 30 *a* and 30 *b*) can be used to study the general dependence of physiological quantities on environmental conditions, although the accuracy of prediction is not known outside the experimental range of ambient air temperatures (18–35°C).

In Table V, predicted rates of respiratory energy loss are given as a function of ambient conditions. At all temperatures, energy loss rate decreases with increasing relative humidity. For moderate and high humidities, energy loss rate decreases with increasing temperature, but at extremely low humidities the energy loss increases slightly with increasing ambient temperature. Rectal temperature, however, has been reported by other investigators to be less strongly dependent, and ventilation rate more strongly dependent (Kleiber, 1961; Carpenter, 1966), on ambient temperature than equations 23, 29 *a*, and 29 *b* imply; this could conceivably cause energy loss rates to decrease with increasing temperature for all relative humidities.

Table VI shows the dependence of respiratory water loss on ambient conditions. For all temperatures, respiratory water loss rate decreases with increasing humidity. Although the effect of lowering the ambient humidity (if temperature is kept constant) is to lower nasal passage temperatures, the decrease in the absolute humidity

TABLE V

PREDICTED RATE OF RESPIRATORY ENERGY TRANSFER AS A FUNCTION OF AMBIENT CONDITIONS

Ambient temp	Ambient relative humidity (%)					
	0	20	40	60	80	100
°C	[cal/(100 g body wt·sec)] × 10^{-3}					
10	6.92	6.65	6.36	6.05	5.74	5.41
12	7.01	6.70	6.37	6.02	5.66	5.29
14	7.10	6.74	6.37	5.97	5.56	5.15
16	7.18	6.77	6.34	5.89	5.44	4.98
18	7.24	6.79	6.31	5.81	5.30	4.79
20	7.31	6.80	6.25	5.70	5.13	4.57
22	7.37	6.79	6.18	5.56	4.94	4.32
24	7.41	6.77	6.10	5.41	4.73	4.05
26	7.44	6.73	5.99	5.24	4.49	3.75
28	7.46	6.68	5.86	5.04	4.23	3.43
30	7.51	6.64	5.74	4.85	3.96	3.09
32	7.55	6.59	5.61	4.63	3.67	2.72
34	7.61	6.52	5.45	4.39	3.34	2.33
36	7.60	6.44	5.27	4.13	3.00	1.90

TABLE VI

PREDICTED RATE OF RESPIRATORY WATER LOSS AS A FUNCTION OF AMBIENT CONDITIONS

Ambient temp	Ambient relative humidity (%)					
	0	20	40	60	80	100
°C	[g water/(100 g body wt·sec)] × 10^{-3}					
10	1.22	1.15	1.08	1.01	0.94	0.87
12	1.24	1.17	1.09	1.01	0.94	0.86
14	1.27	1.18	1.10	1.01	0.93	0.84
16	1.29	1.20	1.10	1.01	0.91	0.81
18	1.31	1.21	1.10	0.99	0.89	0.78
20	1.34	1.22	1.10	0.98	0.87	0.75
22	1.36	1.23	1.09	0.96	0.84	0.71
24	1.37	1.23	1.09	0.94	0.81	0.67
26	1.39	1.23	1.07	0.92	0.77	0.62
28	1.40	1.23	1.06	0.89	0.73	0.57
30	1.42	1.23	1.04	0.86	0.69	0.51
32	1.43	1.23	1.03	0.82	0.64	0.45
34	1.45	1.22	1.01	0.79	0.59	0.39
36	1.46	1.22	0.98	0.75	0.53	0.32

of the expired air is not as great as the decrease in humidity of the inspired air. The effect of ambient humidity on respiratory water loss is greatest at high temperatures; under these conditions an animal may lose four to five times as much water when the humidity is extremely low as it would if the humidity were extremely

high. By staying in its burrow, where the humidity is usually higher than outside (Schmidt-Nielsen and Schmidt-Nielsen, 1950), a kangaroo rat thus gains a substantial reduction in respiratory water loss.

Table VII indicates the dependence of expired air temperature on ambient con-

TABLE VII

PREDICTED NOSE TIP TEMPERATURE AS A FUNCTION OF AMBIENT CONDITIONS

Ambient temp	Ambient relative humidity (%)					
	0	20	40	60	80	100
°C	°C	°C	°C	°C	°C	°C
10	9.8	11.8	13.7	15.3	16.8	18.1
12	10.7	12.9	14.8	16.5	18.1	19.5
14	11.7	14.0	16.0	17.8	19.4	20.9
16	12.6	15.1	17.2	19.1	20.8	22.4
18	13.6	16.2	18.4	20.4	22.2	23.9
20	14.6	17.3	19.7	21.7	23.6	25.3
22	15.6	18.5	21.0	23.1	25.1	26.9
24	16.6	19.6	22.2	24.5	26.5	28.4
26	17.7	20.8	23.5	25.9	28.0	29.9
28	18.8	22.0	24.9	27.3	29.5	31.4
30	19.7	23.2	26.1	28.6	30.9	33.0
32	20.6	24.3	27.4	30.0	32.4	34.5
34	21.6	25.4	28.6	31.4	33.8	36.0
36	22.6	26.6	29.9	32.8	35.3	37.6

TABLE VIII

PREDICTED EFFICIENCY OF VAPOR RECOVERY (DIMENSIONLESS) AS A FUNCTION OF AMBIENT CONDITIONS

Ambient temp	Ambient relative humidity (%)					
	0	20	40	60	80	100
°C						
10	0.755	0.756	0.758	0.760	0.763	0.766
12	0.749	0.750	0.753	0.755	0.758	0.762
14	0.743	0.745	0.747	0.750	0.754	0.757
16	0.736	0.739	0.741	0.745	0.749	0.753
18	0.730	0.732	0.735	0.739	0.743	0.748
20	0.723	0.725	0.729	0.733	0.737	0.743
22	0.715	0.718	0.722	0.726	0.731	0.737
24	0.707	0.710	0.714	0.719	0.725	0.731
26	0.698	0.702	0.706	0.711	0.717	0.724
28	0.688	0.692	0.697	0.703	0.709	0.715
30	0.682	0.686	0.692	0.697	0.703	0.710
32	0.675	0.680	0.685	0.691	0.697	0.704
34	0.667	0.672	0.678	0.684	0.690	0.696
36	0.659	0.665	0.671	0.677	0.682	0.686

ditions. Lowering either ambient temperature or humidity while keeping the other constant has the effect of lowering the expired air temperature. This effect is particularly pronounced at high ambient temperatures and humidities.

Table VIII gives the efficiency of vapor recovery (i.e., the ratio of water recovered on expiration to that evaporated on inspiration). Values of efficiency are within the narrow range of 65–77%. The uniformly high efficiency of vapor recovery is probably quite important in the over-all water economy of the kangaroo rat.

CONCLUSIONS

The model of respiratory heat transfer developed in this study is internally consistent with the data from which it was derived to the extent that expired air temperatures are calculated to within ±0.73°C (SD), the rate of respiratory energy transfer within ±11.1% (SD), and the rate of water loss within ±0.030 (SD). The model, when compared to measurements on additional animals, predicts expired air temperatures within ±1.04°C (SD). Both calculated and predicted values correspond closely with experimental data.

The model can be applied to other small animals for which the various underlying approximations hold. A similar model could be developed for larger animals, but the transverse thermal and vapor transfer in the nasal passages would have to be reconsidered in view of the greater distance from the center of the airstream to the passage wall. Such a model might therefore be more complex than this one, the simplicity of which is one of its advantages.

This work was supported by National Institutes of Health grants HE-05716 and HE-02228, and National Institutes of Health Research Career Award 1-K6-GM-21,522 (K.S.-N.).

Received for publication 24 March 1971.

REFERENCES

CARPENTER, R. E. 1966. *Univ. Calif. Publ. Zool.* **78**:1.

COLLINS, J. 1970. A model of respiratory heat transfer in the kangaroo rat. Ph.D. Dissertation. Duke University, Durham, N. C.

DAVIS, T. P. 1963. *In* Temperature—Its Measurement and Control in Science and Industry. Reinhold Publishing Corp., New York. **3**(Pt. 3):149.

DEPOCAS, F., and J. S. HART. 1957. *J. Appl. Physiol.* **10**:388.

ECKERT, E. R. G., and J. F. GROSS. 1963. Introduction to Heat and Mass Transfer. McGraw-Hill Book Company, New York.

GJÖNNES, B., and K. SCHMIDT-NIELSEN. 1952. *J. Cell. Comp. Physiol.* **39**:147.

GUYTON, A. C. 1947. *Amer. J. Physiol.* **150**:70.

JACKSON, D. C., and K. SCHMIDT-NIELSEN. 1964. *Proc. Nat. Acad. Sci. U. S. A.* **51**:1192.

KAYS, W. M. 1966. Convective Heat and Mass Transfer. McGraw-Hill Book Company, New York.

KLEIBER, M. 1961. The Fire of Life. John Wiley & Sons, Inc., New York.

KREITH, F. 1965. Principles of Heat Transfer. International Textbook Co., New York. 2nd edition.

MERK, H. J. 1958. *Appl. Sci. Res. Sec. A.* **8**:73.

MERRIMAN, M. 1911. A Textbook on the Method of Least Squares. John Wiley & Sons, Inc., New York.

MURRISH, D. E., and K. SCHMIDT-NIELSEN. 1970. *Resp. Physiol.* **10**:151.

QVALE, E. B., and J. L. SMITH, JR. 1969. *J. Eng. Power.* **91**:109.
RAHN, H. 1954. *In* Handbook of Respiratory Physiology. Air University School of Aviation Medicine, Randolph Field, Tex. 29.
ROHSENOW, W. M., and H. CHOI. 1961. Heat, Mass, and Momentum Transfer. Prentice-Hall, Inc. Englewood Cliffs, N. J.
SCHENCK, H. 1959. Heat Transfer Engineering. Prentice-Hall, Inc., Englewood Cliffs, N. J.
SCHLICHTING, H. 1960. Boundary Layer Theory. McGraw-Hill Book Company, New York.
SCHMIDT-NIELSEN, K. 1964. Desert Animals. The Oxford University Press, London.
SCHMIDT-NIELSEN, K., F. R. HAINSWORTH, and D. E. MURRISH. 1970. *Resp. Physiol.* **9**:263.
SCHMIDT-NIELSEN, K., and B. SCHMIDT-NIELSEN. 1950. *Ecology.* **31**:75.
STAHL, W. R. 1967. *J. Appl. Physiol.* **22**:453.
THAUER, R. 1964. *In* Handbook of Physiology. Circulation. American Physiological Society, Washington, D. C. 3(Sec. 2): 1921.
ZIMMERMAN, O. T., and I. LAVINE. 1945. Psychrometric Tables and Charts. Industrial Research Services, Dover, N. H.